P.T. Kuo

DRAFT

A PROBABILISTIC SEISMIC SAFETY ASSESSMENT OF THE DIABLO CANYON NUCLEAR POWER PLANT

by

A. H-S. Ang and N.M. Newmark

84-644

Report to the

U. S. Nuclear Regulatory Commission
Washington, D.C.

N. M. Newmark Consulting Engineering Services
Urbana, Illinois
June 1977

Contents

Foreword

This report represents the result of a study on the evaluation of the seismic safety of the Diablo Canyon nuclear power plant, performed by N. M. Newmark Consulting Engineering Services for the U. S. Nuclear Regulatory Commission.

References to some of the material and publications were provided by Dr. W. J. Hall during the course of the study. The analysis of the seismic hazard was performed with the assistance of Dr. A. Der-Kiureghian.

A PROBABILISTIC SEISMIC SAFETY ASSESSMENT OF THE DIABLO CANYON NUCLEAR POWER PLANT

by

A. H-S. Ang and N. M. Newmark

I. Introduction

1.1 Objectives and Problem Description

The levels of safety against seismic hazards of certain critical components or subsystems of the Diablo Canyon nuclear power plant facility are evaluated quantitatively in terms of the respective annual probability of damage. The evaluations were performed particularly in the light of the recently discovered Hosgri fault, as well as other known fault zones in the region of the plant. At its closest point, the Hosgri fault is approximately six kilometers from the plant.

The power plant is located in an active seismic region of Southern California. A number of fault zones have been identified in the general region within 100 kilometers of the plant, including the San Andreas, the San Simeon, the Rinconada and other faults. The locations of these faults relative to the plant site may be seen in the geographical map of Fig. 1; the shortest surface distances of these various faults to the plant vary from 6 km for the Hosgri to 88 km for the Santa Ynez fault.

The probabilities are determined in terms of the annual probabilities of specific adverse events; these may be the damage of major structural components or pipe joints. However, the event may also be the combined failures of two or more safety related systems whose failure could lead to accidental release of radioactive material; examples of the latter may be the occurrence of a crack in a pipe joint combined with the malfunction of

an electrical shut-off control equipment, or the combination of a pipe break with the malfunction of the emergency core cooling system (ECCS).

1.2 Premise and Special Considerations

The probabilities calculated herein pertain only to the safety of the plant against seismic hazard; no other environmental or man-made hazards are considered aside from that of earthquakes. In this regard, irrespective of the correlations (or lack thereof) between the various components in the plant, they are, of course, all subject to a common environment, namely the earthquake ground motion of the site; consequently the failures of the various components or subsystems in the plant will be (at least) partially correlated, even though the resistances or limiting capacities (fragilities) of the various elements to withstand ground motions may be uncorrelated or statistically independent.

The problem is obviously one of low probability and high consequence. Because such extremely small probabilities are involved, the actual numerical values of the calculated probabilities should not be taken too seriously; only its order of magnitude may be significant. The results of the calculations are intended to provide a quantitative measure of the level of safety underlying the specific components of the plant. The results, however, do not and can not in themselves answer the question of whether or not the plant is safe enough. Nevertheless, the results presented herein should provide a quantitative basis for the resolution of this question.

II. The Probabilistic Approach to Safety Assessment

2.1 Bases of Approach

Failure or damage of a structural component, or safety equipment, would occur when the seismic ground motion exceeds the capability of the component to resist such motions. The maximum ground acceleration that could occur at the site of the power plant over a finite time period is clearly not predictable; similarly, the seismic capability of a major structural component or the fragility limit of a piece of equipment may only be described with a random variable. Consequently, the probability of the resistance being less than the conceivable levels of seismic motions at the site is the relevant measure of safety.

The calculated probabilities must necessarily depend on the bases under which the structural components were designed, and the various safety-related equipments were qualified, for seismic resistances. In this regard, it is stipulated that the major structural components of the Diablo Canyon power plant were designed according to standard practice for the design of nuclear power plant structures, and the class 1 safety equipments were qualified in accordance with recommended practices (e.g. IEEE 1974, 1975).

Because extremely small probabilities are involved, they cannot be estimated directly on the basis of statistical observations, nor verified on the same basis. However, the required probabilities may be deduced through a proper synthesis of available information and statistical data, using established physical relationships of the underlying problem. In this regard, it is important to recognize that the derived probabilities

should be technologically credible, in the sense that it is based on the logical synthesis of various pieces of information, each of which is based on objective data or can be individually judged to be technically sound or reasonable.

In performing the probability calculations, methodologies for determining the seismic hazards (e.g. the maximum ground motions) at the site as well as for determining the description of the resistances are required. The methods used for each of these purposes are described below.

2.2 Determination of Seismic Hazards

Realistically, over a finite time period, it is not possible to state with any percision the maximum ground acceleration that can be expected at the site of the Diablo Canyon power plant. The description of the ground motion intensity may be developed only in terms of probability -- specifically, for example, the probability of exceeding specified acceleration levels in a year, or the annual probability of exceedance.

The site of the power plant is subject to potential earthquake hazards from several well-defined fault systems, including the recently discovered Hosgri fault which is six kilometers offshore from the plant at its closest point. Although all the existing faults in the region are potential sources of earthquakes, the high intensity motions that may be expected at the site would largely be the result of events on the nearby faults, especially the Hosgri. In any case, the total seismic hazard at the site would be the cumulative contributions from all the sources in the region. The determination of these hazards can be performed systematically. In the present case, this determination is based on the recently developed fault-rupture

model of DerKiureghian and Ang (1977). The details of this model will not be described here; it will suffice only to point out the main features of this model.

The DerKiureghian-Ang model is physically consistent with the important characteristics of an earthquake event. It is based on the assumption that an earthquake originates as a fault break at its focus and propagates as an intermittent series of ruptures or slips in the earth's crust, and that the maximum intensity (e.g. acceleration) of ground shaking at the site is determined by the rupture that is closest to the site. Accordingly, the maximum ground acceleration at any point in the neighborhood of an earthquake attenuates with the shortest distance from the rupture. Finally, the occurrence of earthquakes with magnitudes $M \geq 4$ constitutes a Poisson process and, consistent with Richter's magnitude law, the magnitude of an earthquake is described with a truncated exponential distribution (Rosenblueth, 1973).

Schematically, the major fault systems in the region of the Diablo Canyon power plant is depicted in Fig. 1. For each of the faults indicated in Fig. 1, the frequencies of earthquakes of magnitude $M \geq 4$ are assumed to be the same as those observed historically in this region; furthermore, within a given fault, earthquakes are equally likely to occur anywhere along the fault. Also, during a given earthquake, the length of the fault rupture will be a function of the magnitude and appropriate relationship for this purpose must be specified.

The maximum intensity at the plant site, of course, will also depend on the distance to the closest rupture for an earthquake of given magnitude; as illustrated in Fig. 2a, if an earthquake occurs on one of the faults of

such a magnitude as to produce a rupture length ℓ, then the maximum acceleration at the site will be determined by the distance d as shown in Fig. 2a. Besides the hazards of earthquakes from the known faults, earthquakes may occur also anywhere spatially within a hundred-kilometer radius; that is, the epicenter may not necessarily be on one of the known fault systems. Earthquakes from these latter sources are assumed to have fault ruptures that may propogate in any direction from its focus as illustrated in Fig. 2b; the maximum acceleration, however, is still determined by the shortest distance d to the causative fault. Appropriate relationship for the attenuation of the maximum acceleration with d, therefore, will be required.

In using the fault rupture model of DerKiureghian and Ang, a number of physical relationships as well as parameter values must be specified for the site in question. In this regard, the specific relationships and parameter values used for the Diablo Canyon plant site are based on information and data directly pertinent to the site.

With this model, the known physical relationships as well as all historical data of earthquakes and pertinent seismological information are synthesized systematically in a manner consistent with the major characteristics of earthquakes. Of course, the validity of the results will still depend on the reliability of the data and information used with the model to obtain the calculated results. In the present case, the bases for such information and data are described in Sect. 3.1.

On these bases, the total hazards of the Diablo Canyon power plant site is then obtained as the sum of all potential sources within a region of 100 kilometers. The result is the seismic hazard curve representing the annual probability of exceedance associated with specified maximum ground accelerations.

2.3 Determination of Seismic Resistances

The capabilities of the structure and equipments to resist specified levels of ground motions will obviously influence the probability of damage. However, for the purpose of calculating the underlying failure probabilities, it is not necessary to know the actual resistance capability or fragility limit of a specific structural component or piece of equipment; it will be sufficient to know its resistance capability relative to the maximum motion to which it is subjected. This information would be contained in the factors of safety used in the design of the structural components; similarly, the margins or degrees of conservatism underlying the design of the structure or equipment would also provide equivalent information. In other words, one of the parameters required in the determination of the damage probability is the relative value between the median (or mean) value of the resistance to the specified design earthquake (i.e. the safe shutdown earthquake originally prescribed for the design of the plant).

Another resistance parameter that has a bearing on the damage probability is the degree of uncertainty underlying the prediction of resistance, which may be expressed conveniently in terms of the coefficient-of-variation. One of the main tasks, therefore, in the evaluation of the damage probabilities is the assessment of the various sources of uncertainty associated with the prediction of seismic resistance or fragility limits. Available observed data, including information on ranges of observed measurements, may be used in this determination. Invariably, however, the available data and information will be insufficient to provide completely objective bases for assessing the underlying degree of uncertainty. In this light, it will be necessary to augment the available information with engineering

judgment; the necessary judgments, however, may have to be expressed in or translated into probability terms in order to derive the appropriate coefficients-of-variation.

2.4 Calculation of Damage Probability

At a given level of ground acceleration, say a_o, the probability of damage of a component with resistance distribution function $F_R(a)$ would simply be

$$P_F = F_R(a_o) \tag{2.1}$$

which is the area in the probability density function of R below a_o as shown in Fig. 3. However, since there could conceivably be a wide range of possible ground accelerations that may be described as a random variable with probability density function $f_A(a)$, the probability of damage must be integrated over all possible values of a. Hence,

$$P_F = \int_0^\infty F_R(a)\, f_A(a)\, da \tag{2.2}$$

It may be observed that the density function $f_A(a)$ is the negative derivative of the seismic hazard curve shown in Fig. 4a.

Invariably, numerical integration of Eq. 2.2 is necessary; this may be performed as,

$$P_F = \sum_{\text{all a's}} F_R(a) \cdot \Delta F_A(a) \tag{2.3}$$

where,

$$\Delta F_A(a) = F_A(a + \tfrac{\Delta a}{2}) - F_A(a - \tfrac{\Delta a}{2}),$$

is the difference in the ordinates of the hazard curve over a small acceleration interval Δa as shown in Fig. 4a.

In Eq. 2.3, $\Delta F_A(a)$ involves the difference between two small probabilities in the hazard curve; because of the lack of high degree of precision underlying the hazard curve, Eq. 2.3 may accumulate significant error.

An alternative but equivalent formulation for p_F is,

$$p_F = \int_0^\infty [1 - F_A(a)] \cdot f_R(a)\, da \tag{2.4}$$

in which $1-F_A(a)$ is the exceedance probability of acceleration a, as given by the hazard curve of Fig. 4a. Numerically, Eq. 2.4 can be evaluated as,

$$p_F = \sum_{\text{all a's}} [1 - F_A(a)] \cdot \Delta F_R(a) \tag{2.5}$$

where, $\Delta F_R(a) = F_R(a + \frac{\Delta a}{2}) - F_R(a - \frac{\Delta a}{2})$, is the probability that the resistance will be in a small interval Δa, as represented by the incremental area shown in Fig. 4b.

Prescribing the lognormal distribution for the resistance R, we obtain

$$F_R(a) = \phi\left(\frac{\ln a/\bar{r}}{\zeta_R}\right) \tag{2.6}$$

in which $\phi(x)$ is the standard normal probability, and,

$$\zeta_R = \sqrt{\ln(1+\Omega_R^2)} \tag{2.7}$$

where $\bar{r}$ is the median of R; and Ω_R is the coefficient-of-variation representing the uncertainty in R.

The damage probability described above applies to individual components, where $\Delta F_R(a)$ is evaluated for suitable increments of a. However, in the case of a piping system, the failure of any critical section along the pipe would constitute failure of the entire system. In such a case, if there are n independent critical sections in a pipe, the resistance distribution of the piping system would be

$$F_R(a) = 1 - [1-F_1(a)]^n \tag{2.8}$$

in which $F_1(a)$ is the resistance of one critical section.

The incremental probability $\Delta F_R(a)$ then becomes

$$\Delta F_R(a) = n[1-F_1(a)]^{n-1} \cdot \Delta F_1(a) \tag{2.9}$$

Furthermore, it is generally recognized (e.g. WASH 1400) that failure of two or more systems would be necessary to cause release of radioactive material in the plant; for example, the joint failure of the piping system and the electrical safety control equipment. In such a case, the cumulative distribution function of the resistance becomes

$$F_R(a) = \{1 - F_1(a)]^n\} \cdot F_E(a) \tag{2.10}$$

where $F_E(a)$ is the distribution function of the equipment fragility. From which the incremental resistance probability, therefore, is

$$\Delta F_R(a) = \{1 - [1-F_1(a)]^n\} \cdot \Delta F_E(a) + \tag{2.11}$$

$$nF_E(a)\ [1-F_1(a)]^{n-1} \cdot \Delta F_1(a)$$

In Eqs. 2.8 and 2.10, the distribution functions of the respective seismic resistances are also assumed to be lognormal.

III. Pertinent Data and Information Base

As indicated earlier, specific physical relationships and parameter values are needed in the calculation of the required probabilities. The information base used for developing such relationships and for evaluating the specific parameter values are summarized below. In every case, information and data pertinent to the Diablo Canyon site are used for these purposes. However, where objective information is not available or sufficient, subjective judgments are introduced to augment the available information base; when necessary, such judgments would generally tend to be on the conservative side.

3.1 Data for Seismic Hazard Analysis

Obviously, the level of seismic hazard at the Diablo Canyon power plant site would depend on the seismicity of the major faults in the region surrounding the site. The locations of the major faults have been identified geologically; these are summarized in Fig. 1. At the closest point, the surface distances of these faults from the Diablo Canyon plant as well as the lengths of these faults are shown in the table below. Besides the known faults, it is assumed that earthquakes could originate also at any point within a 100-km radius from the plant; fault ruptures from such earthquakes could propagate in any direction. Potential sources within this 100-km radius are represented by the four annular areas described below.

Seismic Source	Surface Distance from site, km	Fault Length, km
San Andreas	75	400
Santa Lucia Bank	48	55
Rinconada-Ozena	30	195
Santa Ynez	88	130
San Simeon	25	132
Hosgri	6	107
Combined Hosgri and San Simeon	6	220
Annular areas:		
1	12	--
2	37	--
3	62	--
4	90	--

Seismicity of Each Fault -- The frequency of significant earthquakes i.e. earthquakes with $M \geq 4$, are different among the various faults in this region. As expected, the average occurrence rate of such earthquakes is highest for the San Andreas fault. In any case, the occurrence rate of significant earthquakes for each of the faults are determined or evaluated on the basis of the epicenter map for this region, as shown in Fig. 5 which is reproduced from Volume II of the Final Safety Analysis Report (1974) for the Diablo Canyon power plant. Fig. 5 represents the epicenter map for this region for the period 1934 through 1971. In the case of the Hosgri, the relocated epicenters reported by Gawthorp (1975) are also used. In evaluating the average occurrence rates for the respective faults, each

epicenter shown in Fig. 5 is assigned to one of the faults within about 5 kilometers. In this way, an actual count of the epicenters for the respective faults are made, from which the average occurrence rate for each fault is then determined. On this basis the annual occurrence rate of $M \geq 4$ for the various faults were obtained as shown in the table below. For the areal sources, the occurrence rates indicated below represent those for each of the annular areas.

Seismic Source	Annual Occurrence Rate of $M \geq 4$	Upper-Bound Magnitude, m_u
San Andreas	6.0	8.0
Santa Lucia Bank	0.92	7.5
Rinconada- Ozena	0.92	7.5
Santa Ynez	0.41	7.5
San Simeon	0.46	7.5
Hosgri	0.22	7.5
Combined Hosgri & San Simeon	0.68	7.5
Annular areas:		
1	0.09	6.5
2	0.27	6.5
3	9.45	6.5
4	5.40	6.5

Frequency Distribution of Magnitude -- The magnitude of significant earthquakes (i.e. with $M \geq 4$) can be described with the shifted exponential distribution (Rosenblueth, 1973), as follows:

$$F_M(m) = k[1 - e^{-\beta(m-4)}]; \qquad 4 \leq m \leq m_u \tag{3.1}$$

where $k = 1-e^{-\beta(m_u-4)}$, in which m_u is the upper-bound magnitude. Because the results could be sensitive to m_u (DerKiureghian and Ang, 1977), reasonable values of m_u must be specified for each of the potential earthquake sources; in the present case, the m_u assigned for the various sources in the region are as shown in the table above.

The parameter β in Eq. 3.1 influences the relative frequencies of different magnitudes, and therefore must also be carefully evaluated. This may be obtained as the slope to the magnitude recurrence curve for the region. The magnitude recurrence curve is a plot of the earthquake magnitude M versus the annual number of events with magnitude greater than or equal to M. The frequency of different earthquake magnitudes in this region has been summarized by Anderson and Trifunac (1976); on the basis of these data, the recurrence line shown in Fig. 6 is developed. The recurrence line shown in Fig. 6 can be observed to be slightly conservative, as it is above almost all of the data points plotted on this figure. The slope of this recurrence line yields a value of $\beta = 2.01$.

The Attenuation Equation -- The attenuation of the maximum acceleration as a function of the shortest surface distance to the fault rupture (or causative fault) is needed with the seismic risk model of DerKiureghian and Ang. For the Southern California region, data of various earthquakes representing the maximum acceleration as a function of the distance to the causative fault for various large-magnitude earthquakes have been reported by Page, et al (1972). These data are summarized in Fig. 7. Page, et al (1972) also observed that the maximum ground acceleration attenuates with the shortest distance d to the slipped fault at a rate of $d^{-1.5}$ to $d^{-2.0}$. On the basis of these data, the following attenuation for maximum acceleration is developed:

$$a = 1.35\, e^{0.67M}(d + 15)^{-1.75} \qquad (3.2)$$

The maximum accelerations given by Eq. 3.2 may be compared with the observed data for this region in Fig. 7. It may be emphasized that in Eq. 3.2, d is the horizontal or surface distance to the slipped fault.

Rupture Length Equation -- The rupture length is obviously a function of the earthquake magnitude. For this purpose, the rupture length equation proposed by Patwardhan, Tocher, and Savage (1975) is used. This relationship can be represented by

$$\ell = 10^{(0.91M - 4.62)} \qquad (3.3)$$

which gives rupture lengths in kilometers. Specific rupture lengths given by Eq. 3.3 for various magnitudes can be seen in the following table.

Magnitude	Rupture Length, km
4	0.1
5	1
6	7
6.5	20
7	56
7.5	160
8	457

3.2 The Seismic Hazard Curve

Using the data described above, and with the DerKiureghian-Ang seismic risk model, the annual probability of exceedance for all levels of ground acceleration (up to 1.5g) are calculated. The result is the seismic hazard curve for the Diablo Canyon power plant site.

Three specific cases were considered as follows:

(1) Considering all seismic sources in the region.

(2) Considering all sources in the region, and assuming that the Hosgri and the San Simeon faults constitute a single fault. This case assumes that the Hosgri is an extention of the San Simeon fault.

(3) Considering only the Hosgri fault. This case calculates the risk associated with earthquakes originating on the Hosgri fault only.

The resulting seismic hazard curves for all the three cases described above are summarized in Fig. 8. The annual exceedance probabilities for specific values of the maximum ground acceleration, ranging from 0 to 1.5g, are also presented in Table 3.1.

The results presented in Fig. 8 also included the effects of the uncertainties underlying the seismic risk model. The most significant of these uncertainties is that associated with the attenuation equation, Eq. 3.2. From the scatter of the observed accelerations shown in Fig. 7, the coefficient-of-variation representing the uncertainty underlying the above attenuation equation is estimated to be around 30%. In short, the hazard curves presented in Fig. 8 has been corrected for the uncertainties associated with the seismic risk model including in particular, the major uncertainty underlying the attenuation equation.

According to the results of the three cases considered herein, the following information (see Fig. 8) may be inferred:

(i) At low levels of acceleration, there is little difference in the seismic risk whether or not the Hosgri is an extention of the San Simeon fault. However, at the higher acceleration levels ($\geq$ 0.5g), there is noticeable difference in the risk between whether the Hosgri and the San Simeon faults are two separate faults or constitute a single longer fault. The difference is about 0.1g for return periods $\geq$ 2500 years.

(ii) For the higher acceleration levels, say $\geq$ 0.5g, the seismic hazard at the Diablo Canyon power plant site is virtually entirely due to the Hosgri fault. At the lower levels of acceleration, the contributions from the other sources are more significant.

3.3 Response and Capacity Determinations

With regard to the evaluation of the structural components, it is the seismic capacity of a component relative to the maximum applied earthquake motion that is relevant. In describing the capacity of a structural component, it will suffice to know the factor of safety used in its design, as this then determines the design capacity relative to the specified design earthquake, normally prescribed as the safe shutdown earthquake (SSE). Structural components of nuclear power plant structures are believed to have an underlying factor of safety that is about three times that for ordinary structures (Newmark, 1975). Thus, the actual factor of safety for nuclear plant structures would be between 10 and 20; i.e., the median seismic resistances would be 10 to 20 times the design earthquake disturbance.

Alternatively, as in the case of equipments, some reserve capacity is normally assured on the basis of qualification tests. According to the IEEE Standards (1974, 1975), light equipments are normally proof-tested for vibrations with maximum acceleration at the equipment mounting that is 10% above that expected during an SSE. The capacities of heavy equipments, however, are determined through calculations. The mean capacities may be determined by assuming that there is a relatively rare chance that an equipment that has been qualified or calculated according to IEEE

standards may fail. In this regard, it will be assumed that light equipments such as electrical or electronic safety control devices will have a failure probability of 0.01, whereas heavy mechanical equipment will be assumed to have an underlying failure probability of 0.001. On this basis and with a specified SSE of 0.4g, the mean seismic capacity of equipments are then determined.

With regard to the seismic capabilities of the piping system, it will be assumed that each critical section of a pipe is designed to withstand the design SSE with an underlying failure probability of 0.001. Pipings and heavy mechanical equipments can undergo some inelastic deformations, and for this reason are ssumed to have a failure probability of 0.001; whereas light electrical equipments probably do not have any reserve ductility and therefore would have a higher failure probability, namely 0.01. Moreover, very high acceleration levels can be expected in the case of light equipments when subjected to the floor spectrum within the plant.

The degree of uncertainty in both the response prediction and capacity determination of the structure as well as the various equipments are also important in evaluating the damage probabilities. The various sources of uncertainty and their combined effects are assessed systematically below.

Uncertainty in Structural Response Prediction and Capacity -- In the case of the structural response prediction, the several sources of uncertainty are as follows:

(i) Effects of Site Dependent Factors on the Definition of Ground Motions -- This would include the effect of local soil conditions and geology on the predicted ground motion at the site as determined by the seismic hazard curve described earlier. Information that can be used to assess the level of uncertainty associated with these factors is scarce.

Based largely on subjective judgment, this uncertainty is estimated to be on the order of 20%, expressed in terms of coefficient-of-variation (c.o.v.).

(ii) Variability in Amplification Factors -- Mohraz, Hall, and Newmark (1972) in their study of a large number of earthquakes have reported the 50 and 90-percentile values of the amplification factors for displacement, velocity, and acceleration; from this study, the 50% and 90% values of the respective amplifications are as follows:

	Disp. Ampl.	Vel. Ampl.	Accel. Ampl.
50% value	1.40	1.66	2.11
90% value	2.21	2.51	2.82

Assuming that the amplification factors can be described as Gaussian random variables, the variabilities for the respective amplifications (expressed in terms of c.o.v.) are:

$$\Omega_d = 45\%$$

$$\Omega_v = 40\%$$

$$\Omega_a = 26\%$$

Therefore, a coefficient-of-variation of 30% to represent the uncertainty associated with the variability in the amplification factor for acceleration appears reasonable and will be used in this study.

(iii) Uncertainty in the Specification of the Structural Damping -- The uncertainty associated with the specification of damping coefficient used in the response calculation of a structure may be of the order of 30%, as has been suggested by Newmark (1974).

(iv) Modeling of Structure for Dynamic Analysis -- Because of the complexity of a nuclear power plant structure, there is bound to be significant uncertainty in modeling the structure for dynamic response analysis.

This should include the effect of structure-soil interaction when pertinent. It is conceivable that this uncertainty could be of the order of 30%, which would include the effects of soil-structure interaction. Since the Diablo Canyon power plant is built on rock, where the effects of soil-structure interaction would not be significant, the 30% assigned herein could be on the conservative side.

On the basis of the individual uncertainty levels assessed above, the total uncertainty associated with the prediction of structural response, therefore, is

$$\Omega_{res} = \sqrt{0.20^2 + 0.30^2 + 0.30^2 + 0.30^2}$$

$$= 0.56.$$

With regard to the uncertainty underlying the estimation of the capacity of the structure or structural component, it is assumed that this uncertainty will be comparable to that associated with the prediction of the resistance to blast forces (Ang, Hall, and Hendron, 1974), which has been estimated to be 30%.

Therefore, the total uncertainty underlying both the response prediction and structural capacity becomes

$$\Omega_{structure} = \sqrt{0.56^2 + 0.3^2} = 0.64$$

From which, the parameter ζ of Eq. 2.7 is,

$$\zeta_{structure} = \sqrt{\ln(1 + 0.64^2)} = 0.59$$

Uncertainty in the Response Prediction and Resistance of Piping Systems -- The forcing function on a piping system would involve the floor response spectra of the structure. Accordingly, any uncertainty in the

prediction of the response of the piping system would be above and beyond those estimated earlier for the structure. This additional uncertainty should include those underlying the in-structure motions such as the floor response spectra that constitute the input to the response analysis of the piping system, as well as any imperfection associated with the modeling and response analysis of the piping system itself. Considering the complexity of pipings in a nuclear power plant, the uncertainty associated with these factors can be expected to be quite large; conceivably, this could range from 30% to 50%. For the purpose of this study, a coefficient-of-variation of 50% will be assumed to represent the level of uncertainty in the prediction of piping system response. Therefore, the total uncertainty associated with the piping system response would be

$$\Omega_{Res} = \sqrt{0.56^2 + 0.50^2} = 0.75$$

With regard to the resistance of a pipe, it is reasonable to assume that pipes can take some inelastic action; for example, it is not unreasonable to expect a ductility factor of 1.5 for pipes. Accordingly, the uncertainty in the resistance of a piping system would be comparable to that of a structural component, and thus a coefficient-of-variation for the piping resistance of 30% may be assigned.

The total uncertainty associated with the response calculation and resistance of a piping system, therefore, is

$$\Omega_{pipe} = \sqrt{0.75^2 + 0.30^2} = 0.81$$

Thus,

$$\zeta_{pipe} = \sqrt{\ell n(1 + 0.81^2)} = 0.71$$

Uncertainty in the Response Prediction and Fragility of Equipment -- In the case of equipments, the additional uncertainty in the in-structure motions as well as in the modeling and response analysis of the equipment would be the same as those of the piping system; these uncertainties, of course, would again be above and beyond those underlying the response prediction of the structure. In other words, a coefficient-of-variation of 50% may also be used for the response prediction of equipment. Accordingly, the uncertainty associated with the response prediction of equipment would also be,

$$\Omega_{res} = \sqrt{0.56^2 + 0.50^2} = 0.75$$

Information on the seismic capacity of equipments are generally proprietary (IEEE Standards, 1974). For this reason, specific information on the fragility limits of equipments used in nuclear power plants are quite rare. However, information on fragility limits of equipments subjected to blast-induced nuclear ground shocks is available Newmark, et al (1963); according to Ang, Hall, and Hendron (1974), the coefficients-of-variation associated with these data are 60% for heavy mechanical equipments, and 80% for light electrical and electronic equipments. It follows then that the total uncertainty underlying the response prediction and fragility of a heavy mechanical equipment is

$$\Omega_{HE} = \sqrt{0.75^2 + 0.60^2} = 0.96$$

From which,

$$\zeta_{HE} = \sqrt{\ln(1 + 0.96^2)} = 0.81$$

Similarly, for light electronic and electrical equipments, the total uncertainty would be

$$\Omega_{LE} = \sqrt{0.75^2 + 0.80^2} = 1.10$$

and,

$$\zeta_{LE} = \sqrt{\ln(1 + 1.10^2)} = 0.89$$

The levels of uncertainties assessed and determined above are summarized in the following; all are expressed in terms of coefficients-of-variation.

Summary of Uncertainties

	Response	Resistance	Total	ζ
Structure	0.56	0.30	0.64	0.59
Piping	0.75	0.30	0.81	0.71
Equipments:				
Heavy Mechanical	0.75	0.60	0.96	0.81
Light Electrical	0.75	0.80	1.10	0.89

IV. Calculated Probabilities

With the formulations described in Chapter 2 and the specific relationships and parameter values described in Chapter 3, the probabilities of specific adverse events involving the damage of major structural components, piping system, or safety equipment, or combinations thereof are evaluated. In all cases, damage is defined to mean that the seismic capacity of the component or equipment is exceeded by the maximum seismic acceleration occurring at the site. Also, in all cases, these probabilities are calculated and presented in terms of the annual probability of damage.

It may be emphasized that the calculated probabilities are based on certain tacit assumptions regarding the manner in which the various components are designed, as described in Chapter III. Such probabilities are necessarily dependent on the criteria under which a component is designed; for example, on the factor of safety and on the safe shut-down earthquake specified in the design of such components. In this regard, a range of design conditions were assumed; specifically, factors of safety ranging from 10 to 20 are assumed to be the conditions under which the major structural components of a nuclear power plant are designed. In the case of equipments, and the piping system, it is more difficult to determine the factors of safety underlying their design; equivalently, however, and for purposes of this calculation, it is assumed that the piping system is designed to withstand the specified SSE of 0.4g with an implied damage probability of 0.001. Similarly, the equipments are assumed to be designed to withstand the specified SSE with an underlying failure probability of 0.01 for light equipments and a failure probability of 0.001 for heavy mechanical equipments.

4.1 Damage of Structural Components

The probability of damage of specific structural components is evaluated using Eq. 2.5, in which $1-F_A(a)$ is the annual seismic hazard curve of Fig. 8 and $F_R(a)$ is assumed to be lognormal.

The results of the calculations are summarized in Table 4.1, which shows the incremental probabilities for accelerations between 0 and 1.5g in increments of 0.12g. The relevant damage probability is then the sum of all these incremental probabilities. In this case, the probability of damage of a major structural component is evaluated for factors of safety of 10 and 20;

also depending on whether the Hosgri and San Simeon faults are separate faults or constitute a single fault, the results are slightly different. The final results can be summarized as follows:

Annual Damage Probability of Structural Component

	Separate Hosgri & San Simeon	Combined Hosgri & San Simeon
Safety Factor = 10	1.29×10^{-6}	1.88×10^{-6}
Safety Factor = 20	3.31×10^{-8}	5.12×10^{-8}

The respective contribution to the total damage probability from the different ranges of ground accelerations can be seen in Figs. 9 and 10; the step size shown in these figures represent the incremental probabilities associated with the respective acceleration increments. On this basis, the range of ground accelerations that has major contributions to the damage probability may be observed.

It may be emphasized that the probabilities calculated above pertain to the damage of individual structural components. In general, it does not necessarily mean the collapse of the component. Moreover, in the case of redundant structures, the damage of a single structural component may not be of serious consequence to the structural system. However, common design and construction procedures, plus stringent inspection requirements to achieve uniform resistance quality, would tend to increase the correlation between the resistances of various components. For this reason, damage to one structural component may likely cause similar damage to other components in the same structure.

4.2 Damage of Piping System

In the case of a piping system, the resistance along the length of a pipe will generally be correlated; however, because there are numerous

welded connections of a piping system in a nuclear power plant, many of which could be potential locations of weakness, it is likely that some of the pipe sections may be uncorrelated. In a given piping system, it is probably reasonable to stipulate that there could be several, say n, independent sections of potential failure locations in the system. Clearly, the occurrence of damage (for example, the occurrence of a macro crack at a welded joint) in one section is tantamount to failure of the piping system; hence failure in this case is determined by the weakest among the n independent sections. Accordingly, therefore, for the piping system, the resistance distribution function would be defined by Eq. 2.8, in which $F_1(a)$ is the distribution function of the resistance of one pipe section.

The value of n would probably range between 1 and 10. Calculations for n = 1, 5, and 10 are summarized in Table 4.2. Again, the incremental probabilities in each case are shown in Table 4.2 for accelerations ranging from 0 to 1.5g in increments of 0.12g. The respective damage probabilities is the sum of all the incremental probabilities. It can be observed on the basis of the results summarized in Table 4.2 that the damage probability of the piping system, depending on the value of n, is as follows:

n	Separate Hosgri & San Simeon	Combined Hosgri & San Simeon
1	4.08×10^{-6}	5.96×10^{-6}
5	1.96×10^{-5}	2.86×10^{-5}
10	3.76×10^{-5}	5.46×10^{-5}

In the case of the piping system in a nuclear power plant, it is probably realistic and reasonable to assume a value of n = 5. On this basis, then the damage probability of the piping system would be of the order of 10^{-5} annually.

The incremental probabilities representing the contributions to the total damage probability from the various acceleration increments are portrayed in Fig. 11 (for n = 1).

4.3 Piping Damage and Malfunction of Light Equipment

An adverse event that may likely lead to release of radioactive material is the joint occurrence of damage somewhere along the piping system and the failure or malfunction of the safety control equipment. The probability of this joint event can be calculated assuming that the resistances of the piping system and the control equipment are statistically independent, but are subject to the common seismic environment of ground acceleration. In this case, therefore, the joint resistance distribution function is given by Eq. 2.10.

Again, three values of n for the piping system are used in the calculations. The results are summarized in Table 4.3, which shows the incremental probabilities for all levels of ground acceleration, yielding the annual probability of this joint event for three values of n as follows:

$$n = 1; \quad P_F = 3.01 \times 10^{-7}$$

$$n = 5; \quad P_F = 1.40 \times 10^{-6}$$

$$n = 10; \quad P_F = 2.57 \times 10^{-6}$$

These probabilities were obtained assuming that the Hosgri and San Simeon faults are separate faults.

The relative contributions to the total damage probability from the various increments of ground acceleration can be seen from the different step size of the curve in Fig. 12.

4.4 Piping Damage and Failure of Heavy Equipment

Another adverse event of concern is the joint occurrence of a major pipe damage somewhere in the piping system of the plant and the simultaneous malfunction of certain heavy safety equipment such as the emergency core cooling system (ECCS). The calculations involved here are similar to those described in Sect. 4.3, with the exception that for a heavy mechanical equipment such as the ECCS, it is assumed that the equipment is designed to withstand the SSE of 0.4g with an underlying failure probability of 0.001, in contrast to 0.01 for a light equipment.

The results of the calculations are summarized for this case in Table 4.4, showing the incremental probabilities for the entire range of accelerations of interest. In this case, the probability of this adverse event, for the three values of n, are as follows:

$$n = 1; \quad P_F = 8.39 \times 10^{-8}$$
$$n = 5; \quad P_F = 3.85 \times 10^{-7}$$
$$n = 10; \quad P_F = 6.97 \times 10^{-7}$$

The results for n = 1 are also portrayed in Fig. 13, showing the relative contributions to the total damage probability from the different acceleration increments.

V. Summary

Seismic safety of the Diablo Canyon nuclear power plant has been systematically evaluated, in terms of the annual probabilities of adverse events involving the damage or malfunction of one or more components in the plant; such events are those that could potentially lead to release

of radioactive material. The specific events and associated probabilities can be summarized as follows:

Damage to Structural Components -- 3.3×10^{-8} for safety factor = 20; to 1.3×10^{-6} for safety factor = 10.

Damage to Piping System -- 4.0×10^{-6} for n = 1; to 3.8×10^{-5} for n = 10.

Damage to Piping and Malfunction of Light Electrical Equipment -- 3.0×10^{-7} for n = 1; to 2.6×10^{-6} for n = 10.

Damage to Piping and Malfunction of ECCS -- 8.4×10^{-8} for n = 1; to 7.0×10^{-7} for n = 10.

The probabilities calculated herein pertain to all levels of potential earthquake hazards at the site. In obtaining these probabilities, a careful analysis of the seismic hazard for the site was performed using a fault-rupture model for this purpose, giving the probability of exceedance for all significant ground accelerations expected at the site. Also, a careful analyes of the seismic resistances of major structural components and equipments were performed, including an assessment of the uncertainties underlying the respective resistance functions. The relevant probabilities are then evaluated by integrating the damage probabilities associated with all accelerations from 0 to 1.5g.

References

1. Anderson, J. G., and Trifunac, M. C., "Uniform Risk Absolute Acceleration Spectra for the Diablo Canyon Site, California," Rept. to the ACRS, U.S. Nuclear Regulatory Commission, 1976.

2. Ang, A. H-S., Hall, W. J., and Hendron, A. J., "Uncertainty and Survivability Evaluations of Design to Air-Blast and Ground Shock," Final Report Contract DACA 88-73-C-0040 to U.S. Army Construction Engineering Research Laboratory, June 1974.

3. Der-Kiureghian, A., and Ang, A. H-S., "A Fault-Rupture Model for Seismic Risk Analysis," Bulletin, Seismological Society of America, August 1977.

4. Inst. of Electrical and Electronics Engineers, Inc.,"IEEE Standard for Qualifying Class IE Equipment for Nuclear Power Generating Stations," IEEE Std. 323-1974, 1974.

5. Inst. of Electrical and Electronics Engineers, "IEEE Recommended Practices for Seismic Qualification of Class 1E Equipment for Nuclear Power Generating Stations," IEEE Std. 344-1975, 1975.

6. Mohraz, B., Hall, W. J., and Newmark, N. M., "A Study of Vertical and Horizontal Earthquake Spectra," Contract AT(49-5)-2667, Atomic Energy Commission, N. M. Newmark Consulting Engineering Services, Dec. 1972.

7. Newmark, N. M., "Comments on Conservatism in Earthquake Resistant Design," Report to U.S. Nuclear Regulatory Commission, Sept. 1974.

8. Newmark, N. M., "Probability of Predicted Seismic Damage in Relation to Nuclear Reactor Facility Design," Draft Rept. to Nuclear Regulatory Commission, Contract AT(49-24)-0116, N. M. Newmark Consulting Engineering Services, Sept. 1975.

9. Newmark, Hansen, and Associates, "Vulnerability Handbook for Hardened Installations," Vol. I, Final Rept. Contract AF 33(657)-10287, Dec. 1963.

10. Pacific Gas and Electric, Final Safety Analysis Report, Units 1 and 2 of Diablo Canyon Site, Vol. II, USAEC Docket Nos. 50-275 and 50-323, 1974.

11. Page, R. A., Boore, D. M., Joyner, W. B., and Coulter, H. W., "Ground Motion Values for Use in the Seismic Design of the Trans-Alaska Pipeline System," Geological Survey Circular 672, 1972.

12. Patwardhan, A. S., Tocher, D., and Savage, E. D., "Relationship Between Earthquake Magnitude and Length of Rupture Surface Based on Aftershock Zones," 70th Annual Mtg., Seismological Soc. of Am., Earthquake Notes, Eastern Section, Vol. 46, No. 3, July-Sept. 1975.

13. Rosenblueth, E., "Analysis of Risk," Proc. 5th World Conf. on Earthquake Engineering, Rome, Italy, 1973.

Table 3.1 Annual Probability of Exeedance

Annual Max. Ground Accel., g	All Sources		Hosgri Only
	Separate Hosgri & San Simeon	Combined Hosgri & San Simeon	
0.10	5.1×10^{-2}	6.0×10^{-2}	1.6×10^{-2}
0.20	7.5×10^{-3}	9.2×10^{-3}	3.0×10^{-2}
0.30	1.9×10^{-3}	2.4×10^{-3}	1.0×10^{-3}
0.40	7.5×10^{-4}	1.0×10^{-3}	5.0×10^{-4}
0.50	3.6×10^{-4}	5.3×10^{-4}	2.9×10^{-4}
0.60	2.0×10^{-4}	3.1×10^{-4}	1.8×10^{-4}
0.70	1.2×10^{-4}	1.9×10^{-4}	1.2×10^{-4}
0.75	9.8×10^{-5}	1.5×10^{-4}	9.5×10^{-5}
0.80	7.8×10^{-5}	1.2×10^{-4}	7.7×10^{-5}
0.90	5.1×10^{-5}	7.9×10^{-5}	5.1×10^{-5}
1.00	3.2×10^{-5}	5.0×10^{-5}	3.2×10^{-5}
1.10	2.1×10^{-5}	3.2×10^{-5}	2.1×10^{-5}
1.20	1.2×10^{-5}	1.9×10^{-5}	1.2×10^{-5}
1.30	7.4×10^{-6}	1.1×10^{-5}	7.4×10^{-5}
1.40	5.0×10^{-6}	7.2×10^{-6}	5.0×10^{-6}
1.50	2.7×10^{-6}	4.2×10^{-6}	2.7×10^{-6}

Table 4.1 Damage Probability of Structure

Δp_F

	Separate Hosgri & San Simeon		Combined Hosgri & San Simeon	
Accel., g	F.S. = 10	F.S. = 20	F.S. = 10	F.S. = 20
0.12	2.341×10^{-9}	1.590×10^{-12}	2.765×10^{-9}	1.879×10^{-12}
0.24	2.166×10^{-8}	5.052×10^{-11}	2.743×10^{-8}	6.400×10^{-11}
0.36	6.380×10^{-8}	2.937×10^{-10}	8.612×10^{-8}	3.964×10^{-10}
0.48	1.136×10^{-7}	8.818×10^{-10}	1.638×10^{-7}	1.272×10^{-9}
0.60	1.595×10^{-7}	1.888×10^{-9}	2.404×10^{-7}	2.845×10^{-9}
0.72	1.899×10^{-7}	3.193×10^{-9}	2.924×10^{-7}	4.917×10^{-9}
0.84	1.960×10^{-7}	4.451×10^{-9}	3.043×10^{-7}	6.910×10^{-9}
0.96	1.765×10^{-7}	5.210×10^{-9}	2.749×10^{-7}	8.111×10^{-9}
1.08	1.419×10^{-7}	5.317×10^{-9}	2.212×10^{-7}	8.285×10^{-9}
1.20	1.050×10^{-7}	4.788×10^{-9}	1.637×10^{-7}	7.465×10^{-9}
1.32	7.174×10^{-8}	3.968×10^{-9}	1.119×10^{-7}	6.188×10^{-9}
1.44	4.636×10^{-8}	3.048×10^{-9}	7.234×10^{-8}	4.756×10^{-9}
p_F =	1.288×10^{-6}	3.309×10^{-8}	1.961×10^{-6}	5.121×10^{-8}

Table 4.2 Damage Probability of Piping

Δp_F

Accel., g	Separate Hosgri & San Simeon			Combined Hosgri & San Simeon		
	n=1	n=5	n=10	n=1	n=5	n=10
0.12	1.591×10^{-7}	8.030×10^{-7}	1.605×10^{-6}	1.897×10^{-7}	9.487×10^{-7}	1.897×10^{-6}
0.24	4.043×10^{-7}	2.021×10^{-6}	4.042×10^{-6}	5.123×10^{-7}	2.561×10^{-6}	5.121×10^{-6}
0.36	5.507×10^{-7}	2.750×10^{-6}	5.492×10^{-6}	7.433×10^{-7}	3.712×10^{-6}	7.413×10^{-6}
0.48	5.844×10^{-7}	2.908×10^{-6}	5.781×10^{-6}	8.427×10^{-7}	4.193×10^{-6}	8.336×10^{-6}
0.60	5.699×10^{-7}	2.813×10^{-6}	5.534×10^{-6}	8.590×10^{-7}	4.239×10^{-6}	8.340×10^{-6}
0.72	5.153×10^{-7}	2.506×10^{-6}	4.842×10^{-6}	7.934×10^{-7}	3.859×10^{-6}	7.455×10^{-6}
0.84	4.312×10^{-7}	2.052×10^{-6}	3.856×10^{-6}	6.693×10^{-7}	3.184×10^{-6}	5.985×10^{-6}
0.96	3.282×10^{-7}	1.515×10^{-6}	2.741×10^{-6}	5.111×10^{-7}	2.358×10^{-6}	4.267×10^{-6}
1.08	2.323×10^{-7}	1.032×10^{-6}	1.778×10^{-6}	3.620×10^{-7}	1.607×10^{-6}	2.771×10^{-6}
1.20	1.529×10^{-7}	6.475×10^{-7}	1.053×10^{-6}	2.385×10^{-7}	1.010×10^{-6}	1.641×10^{-6}
1.32	9.554×10^{-8}	3.829×10^{-7}	5.808×10^{-7}	1.490×10^{-7}	5.972×10^{-7}	9.058×10^{-7}
1.44	5.666×10^{-8}	2.132×10^{-7}	2.988×10^{-7}	8.842×10^{-8}	3.326×10^{-7}	4.662×10^{-7}
p_F =	4.081×10^{-6}	1.964×10^{-5}	3.760×10^{-5}	5.960×10^{-6}	2.860×10^{-5}	5.460×10^{-5}

Table 4.3 Piping and Light Equipment Damage Probability

	ΔP_F		
Accel., g	n = 1	n = 5	n = 10
0.12	2.498×10^{-11}	1.249×10^{-10}	7.854×10^{-9}
0.24	1.154×10^{-9}	5.771×10^{-9}	1.154×10^{-8}
0.36	6.287×10^{-9}	3.141×10^{-8}	6.274×10^{-8}
0.48	1.572×10^{-8}	7.831×10^{-8}	1.559×10^{-7}
0.60	2.781×10^{-8}	1.376×10^{-7}	2.715×10^{-7}
0.72	3.931×10^{-8}	1.922×10^{-7}	3.738×10^{-7}
0.84	4.650×10^{-8}	2.233×10^{-7}	4.248×10^{-7}
0.96	4.705×10^{-8}	2.205×10^{-7}	4.070×10^{-7}
1.08	4.184×10^{-8}	1.901×10^{-7}	3.378×10^{-7}
1.20	3.345×10^{-8}	1.463×10^{-7}	2.485×10^{-7}
1.32	2.471×10^{-8}	1.034×10^{-7}	1.669×10^{-7}
1.44	1.699×10^{-8}	6.772×10^{-8}	1.032×10^{-7}
P_F =	3.009×10^{-7}	1.397×10^{-6}	2.572×10^{-6}

Table 4.4 Piping and Heavy Equipment Damage Probability

	Δp_F		
Accel., g	n=1	n=5	n=10
0.12	6.030×10^{-13}	3.015×10^{-12}	6.030×10^{-12}
0.24	7.086×10^{-11}	3.542×10^{-10}	7.084×10^{-10}
0.36	6.379×10^{-10}	3.187×10^{-9}	6.366×10^{-9}
0.48	2.226×10^{-9}	1.109×10^{-8}	2.207×10^{-8}
0.60	5.034×10^{-9}	2.492×10^{-8}	4.920×10^{-8}
0.72	8.580×10^{-9}	4.200×10^{-8}	8.180×10^{-8}
0.84	1.184×10^{-8}	5.701×10^{-8}	1.088×10^{-7}
0.96	1.357×10^{-8}	6.381×10^{-8}	1.183×10^{-7}
1.08	1.352×10^{-8}	6.177×10^{-8}	1.106×10^{-7}
1.20	1.185×10^{-8}	5.225×10^{-8}	8.967×10^{-8}
1.32	9.499×10^{-9}	4.021×10^{-8}	6.581×10^{-8}
1.44	7.027×10^{-9}	2.842×10^{-8}	4.414×10^{-8}
p_F =	8.386×10^{-8}	3.850×10^{-7}	6.971×10^{-7}

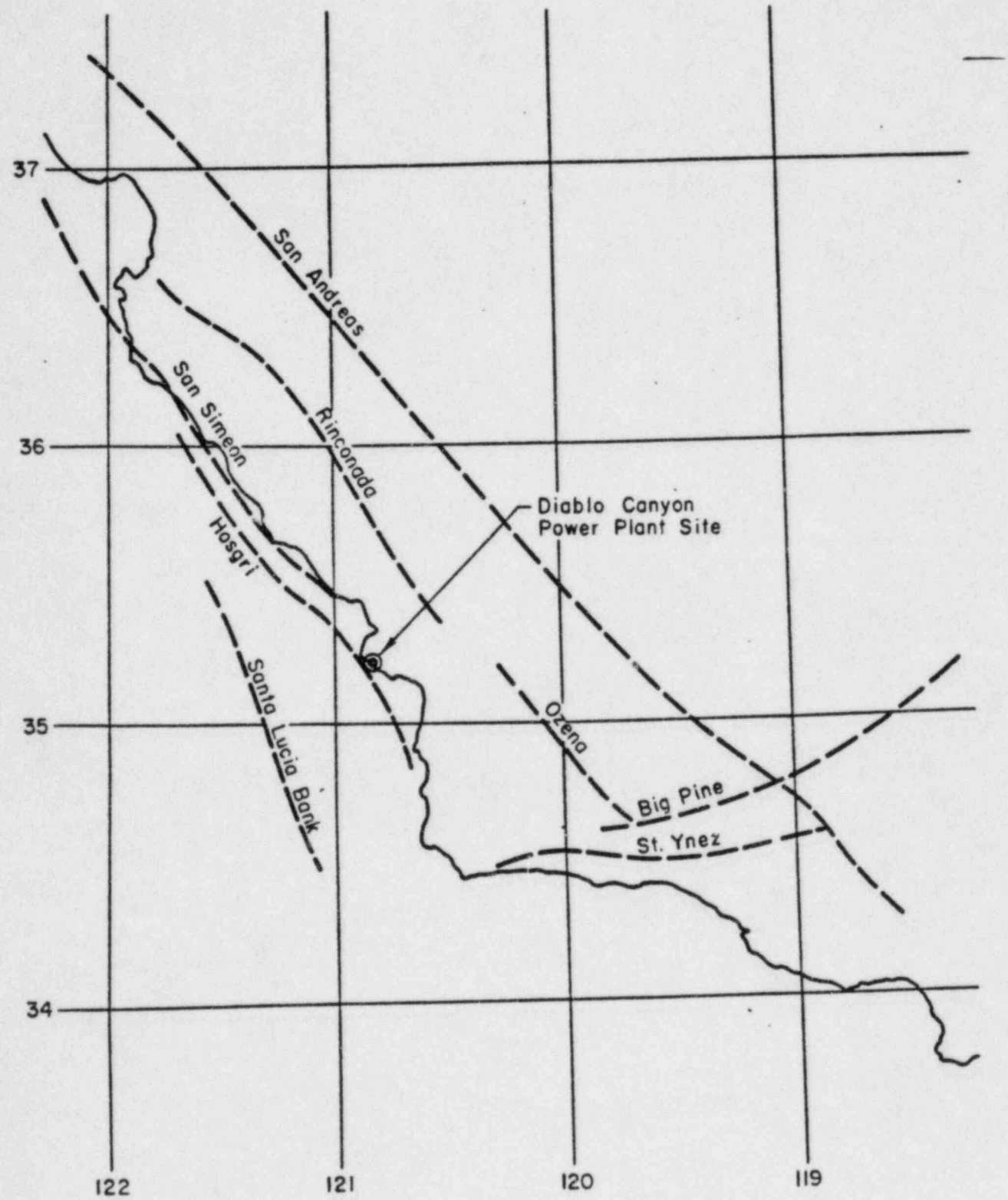

FIG. 1 MAJOR FAULTS IN REGION OF SITE

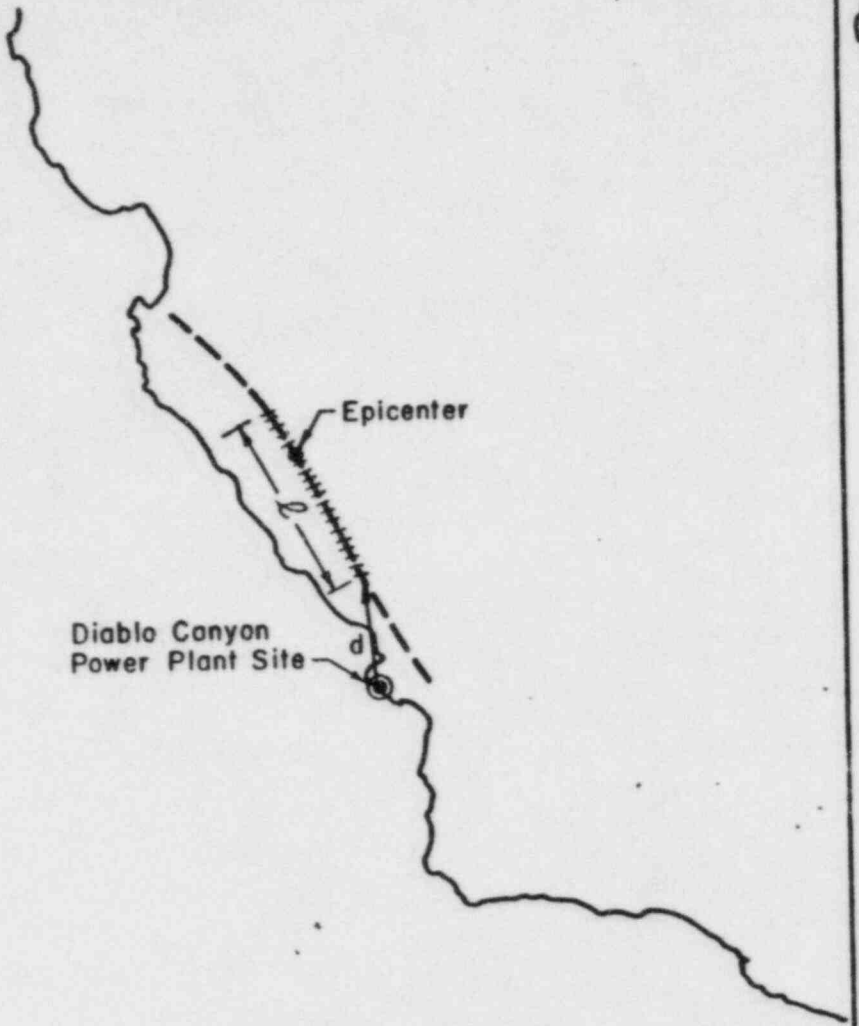

FIG. 2a EARTHQUAKE ON A KNOWN FAULT

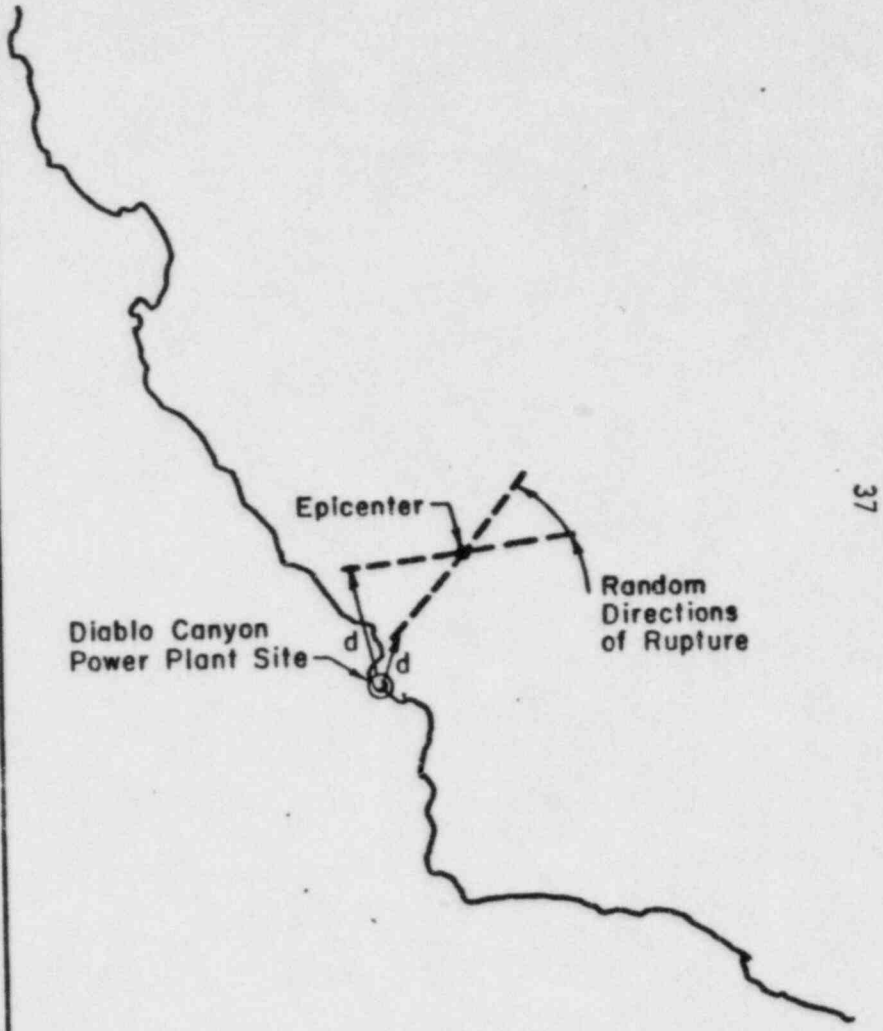

FIG. 2b EARTHQUAKE NOT ON A FAULT

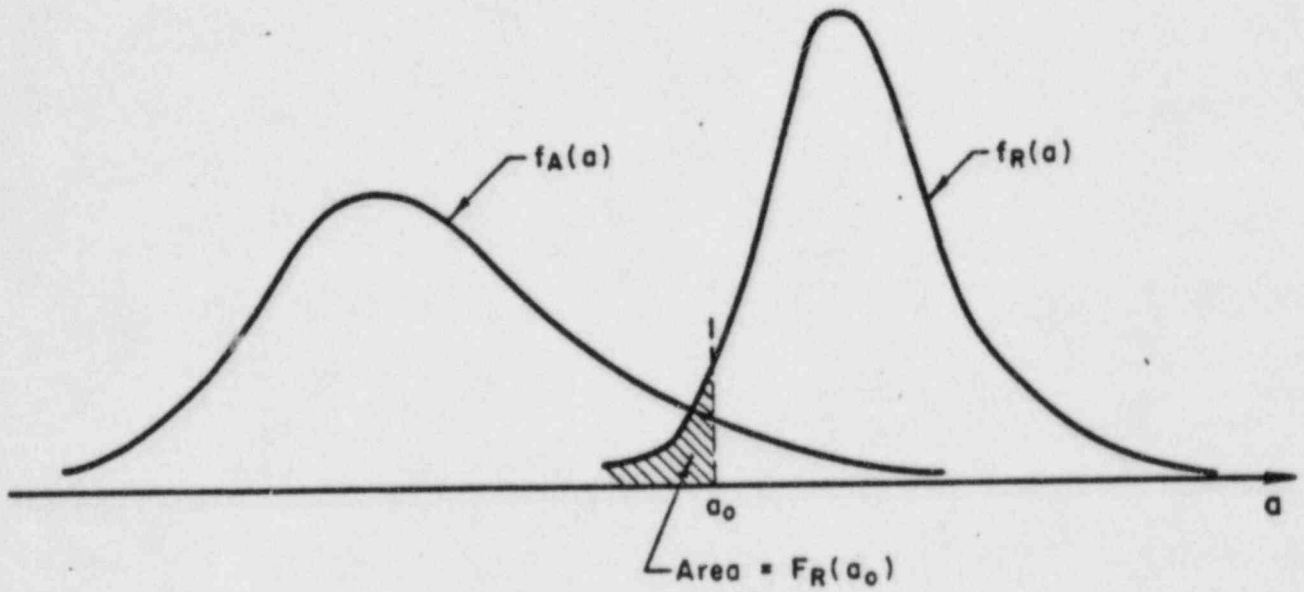

FIG. 3 PROBABILITY DENSITY FUNCTIONS

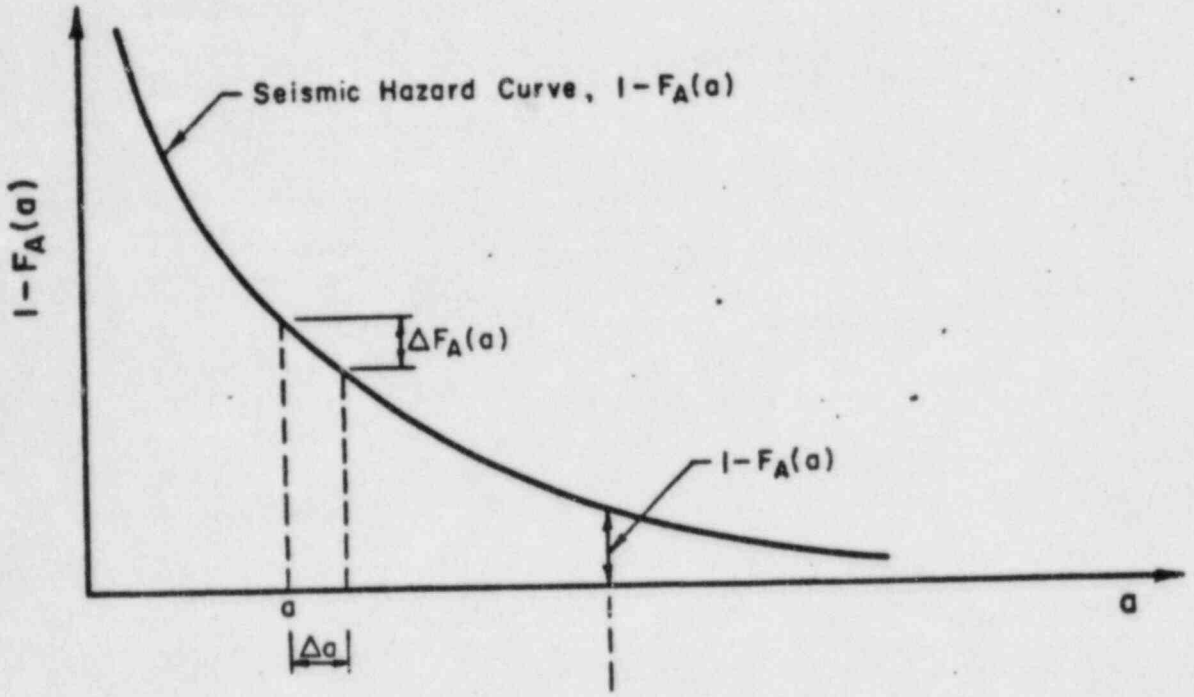

FIG. 4a SEISMIC HAZARD CURVE

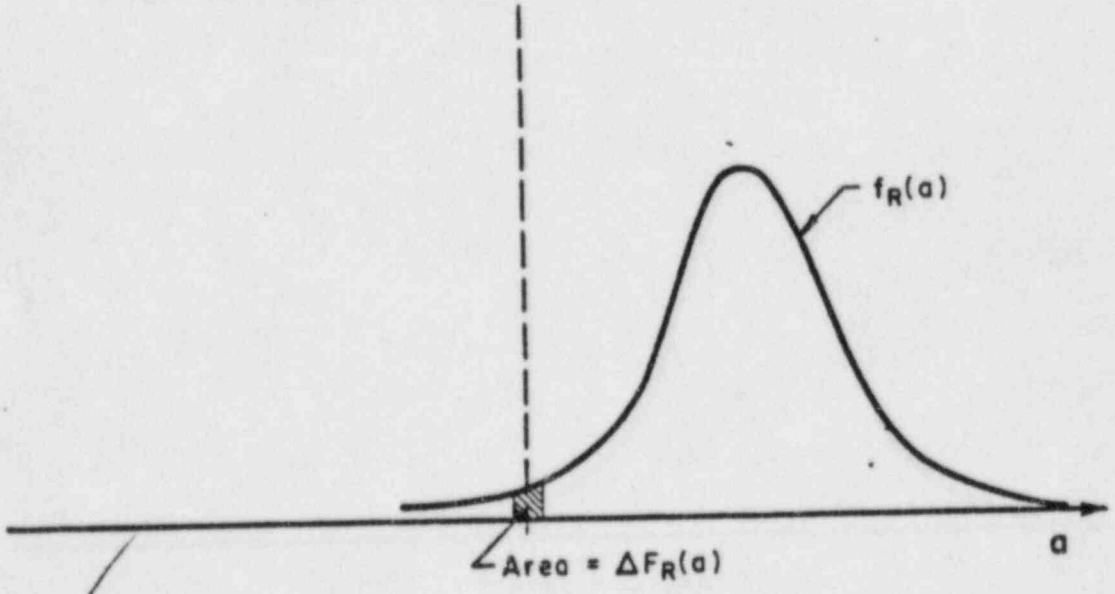

FIG. 4b RESISTANCE DENSITY FUNCTION

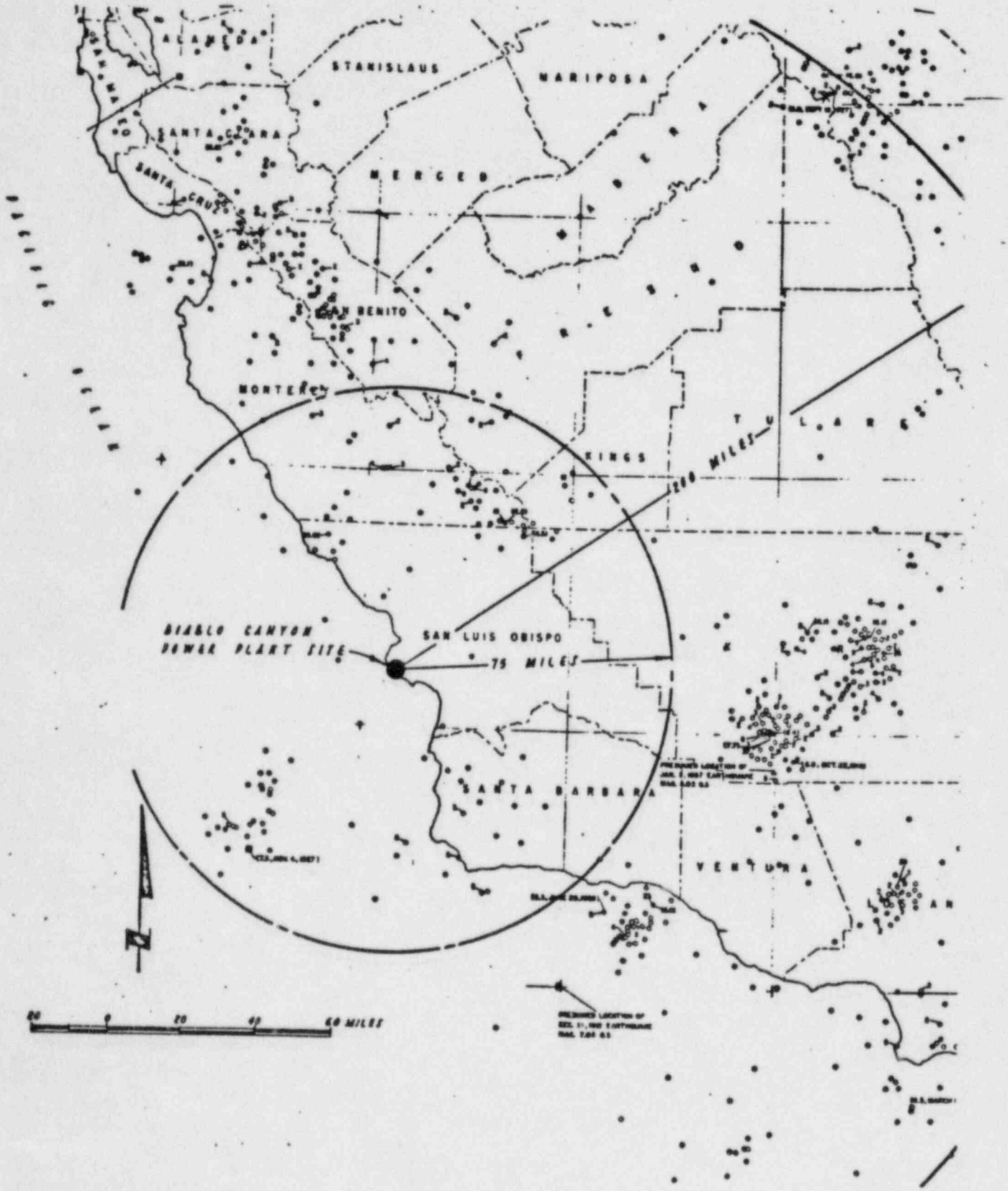

FIG. 5 EPICENTER MAP OF REGION

(Reproduced from Final Safety Analysis Report for Diablo Canyon Plant)

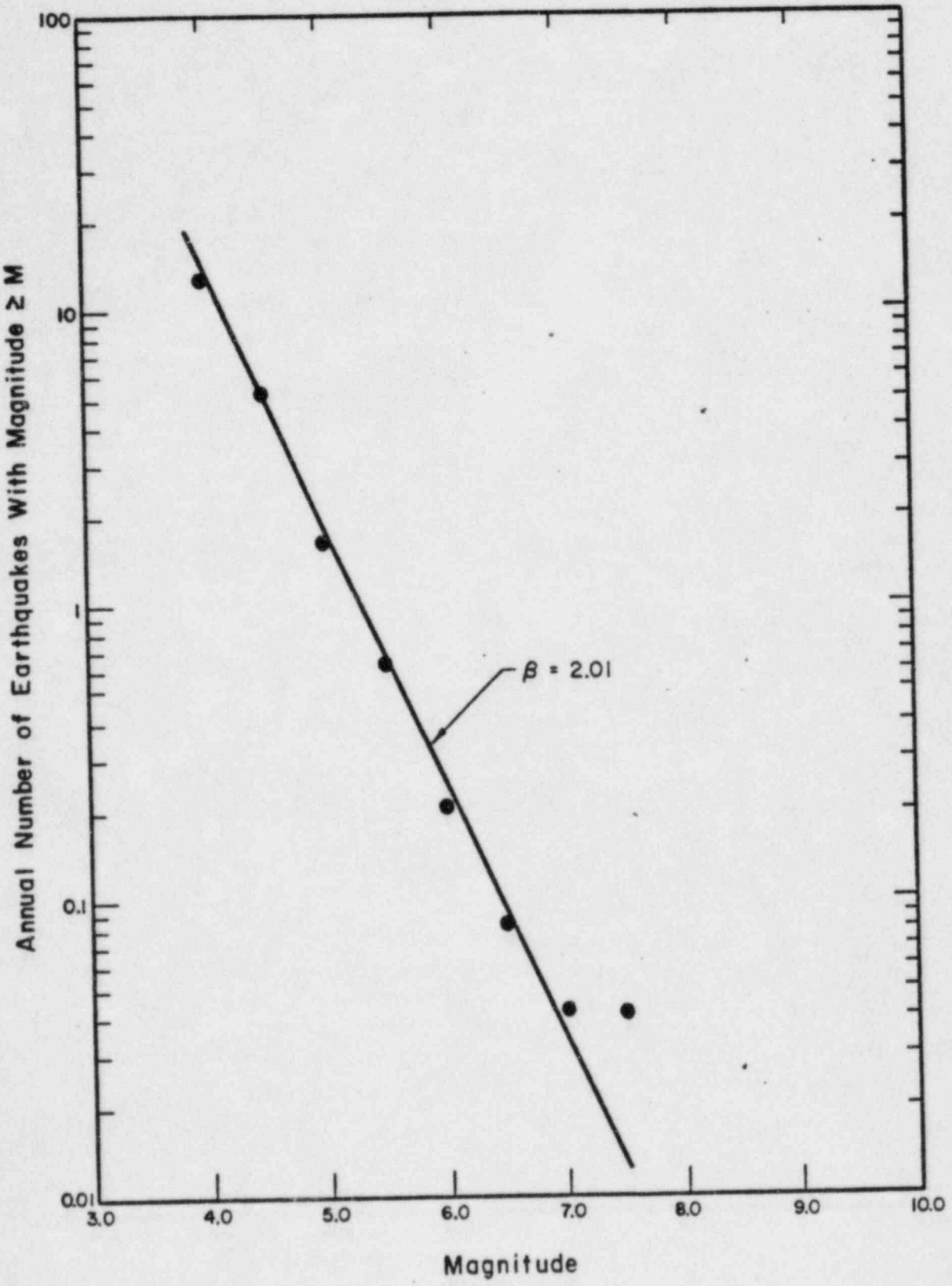

FIG. 6 MAGNITUDE RECURRENCE CURVE

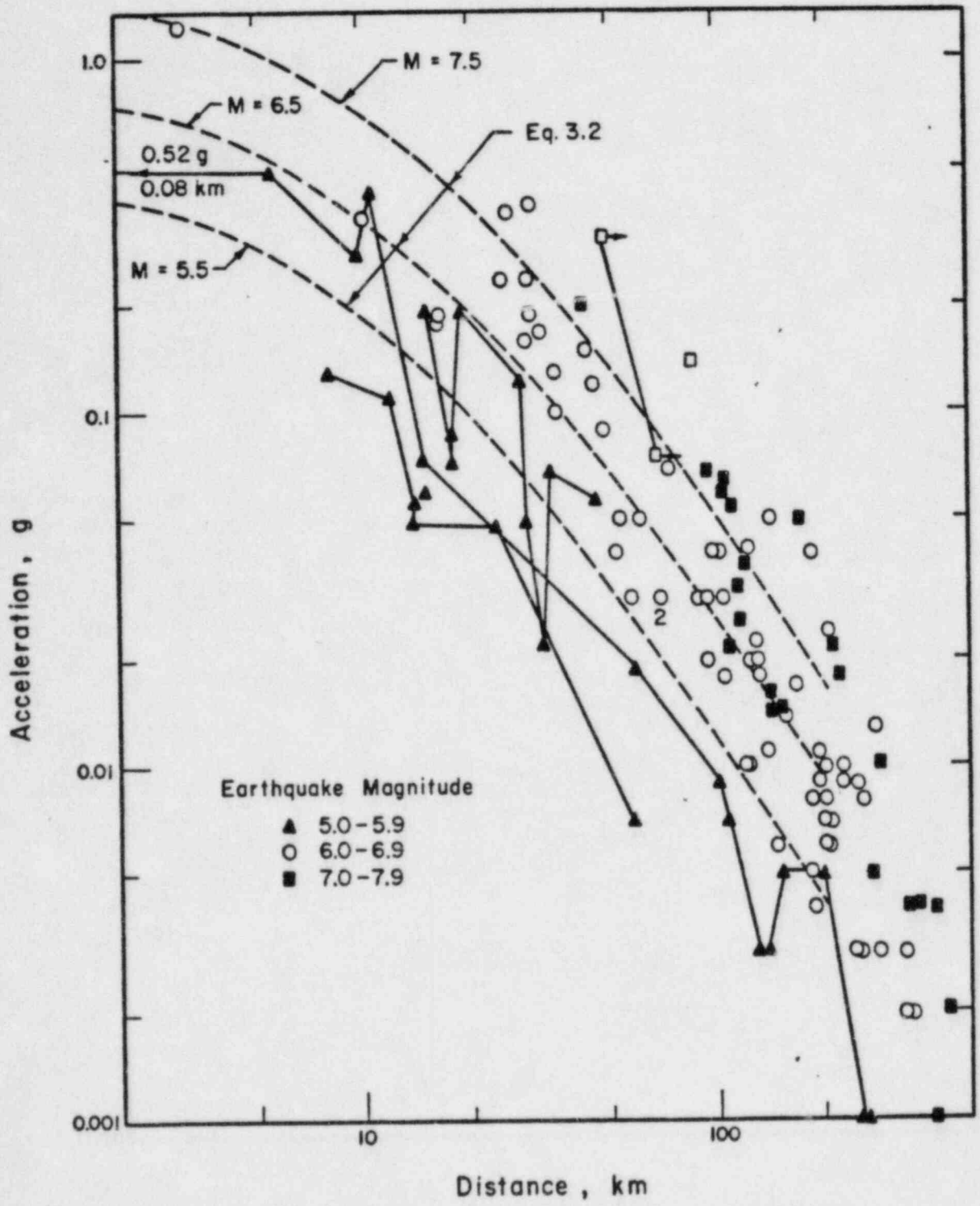

FIG. 7 ATTENUATION OF MAXIMUM ACCELERATION WITH DISTANCE TO SLIPPED FAULT (DATA REPRODUCED FROM PAGE, et al, 1972)

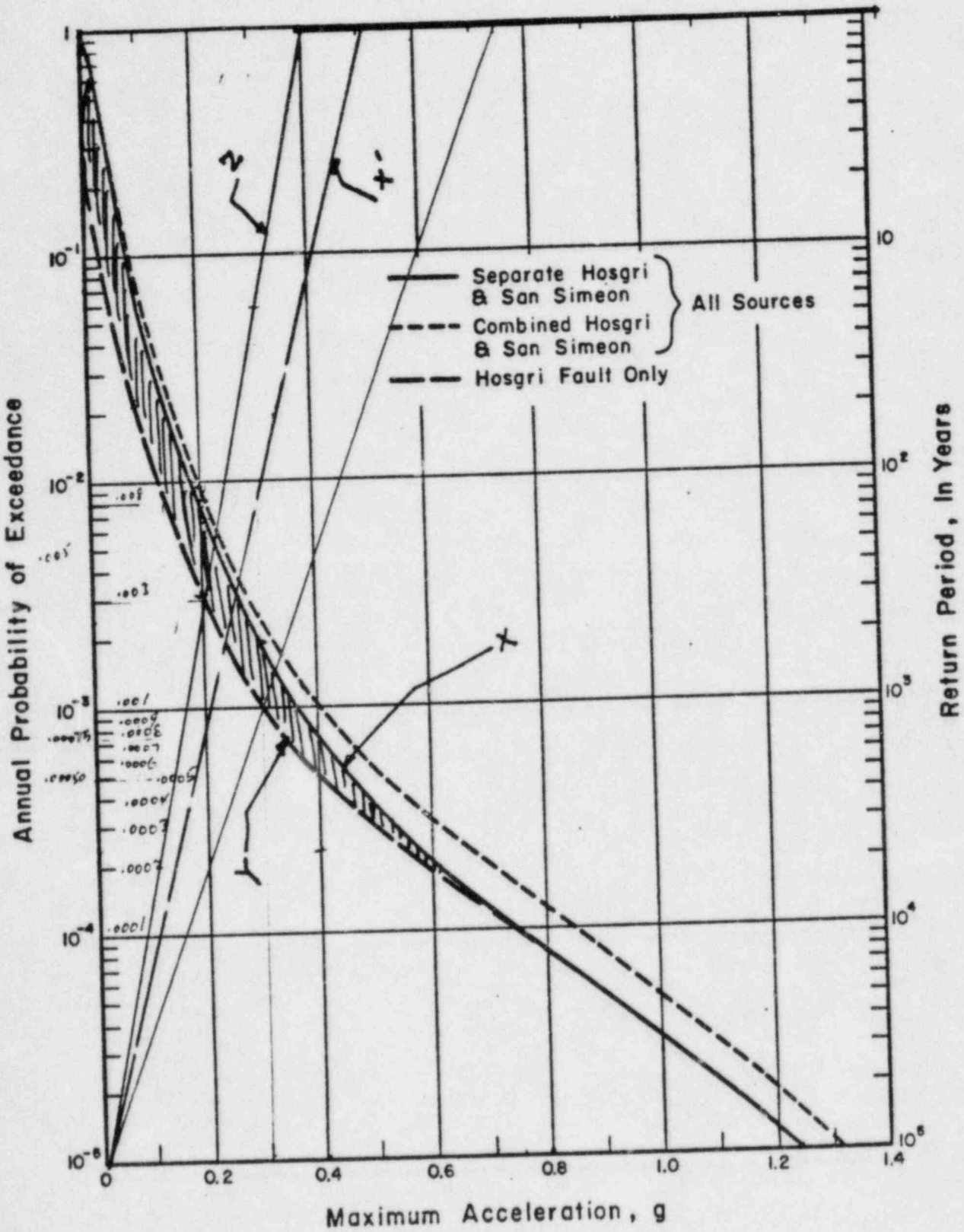

FIG. 8 SEISMIC HAZARD CURVES FOR DIABLO CANYON POWER PLANT SITE

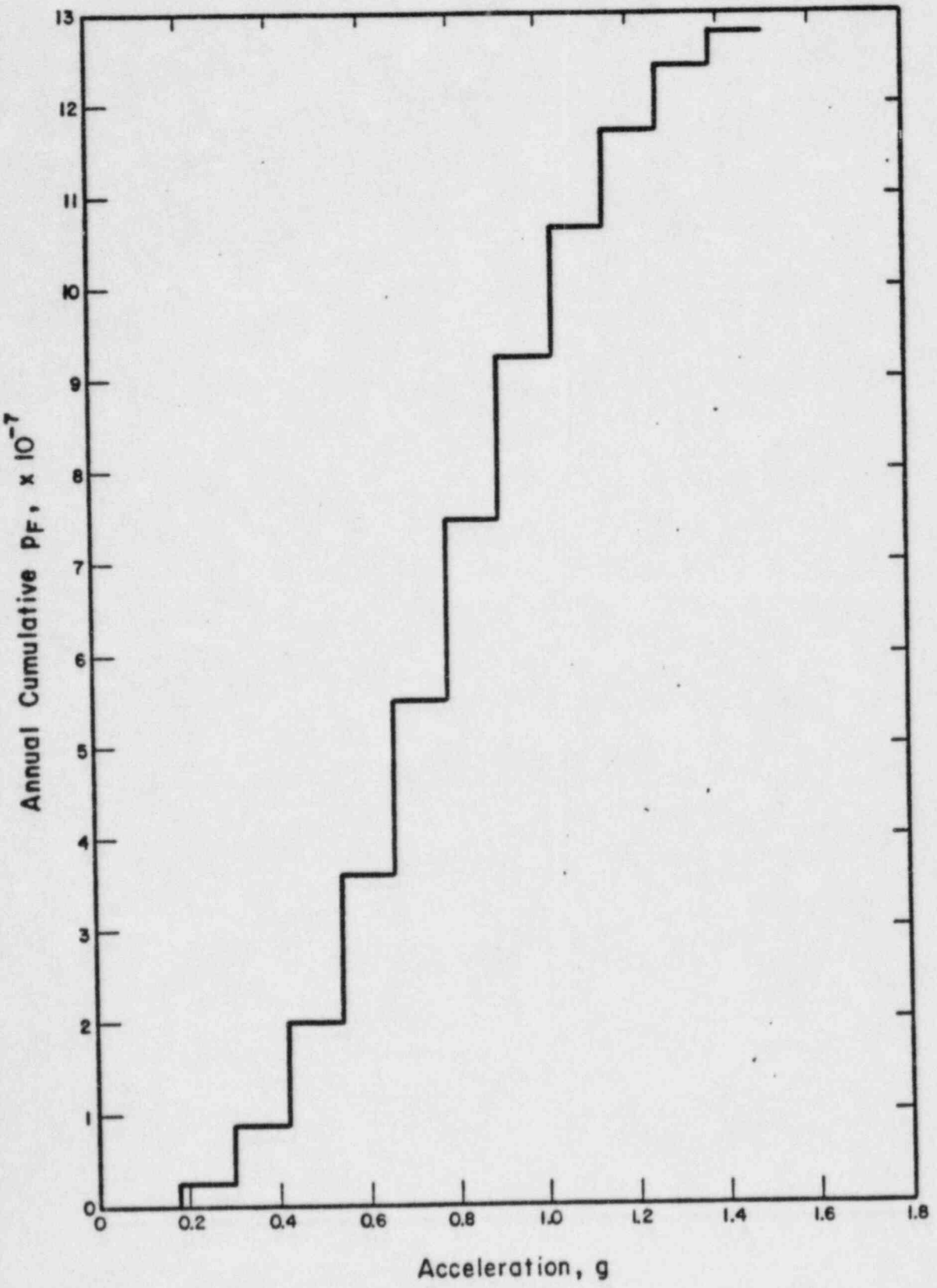

FIG. 9 INCREMENTAL CONTRIBUTIONS TO DAMAGE PROBABILITY OF STRUCTURAL COMPONENT (SF = 10)

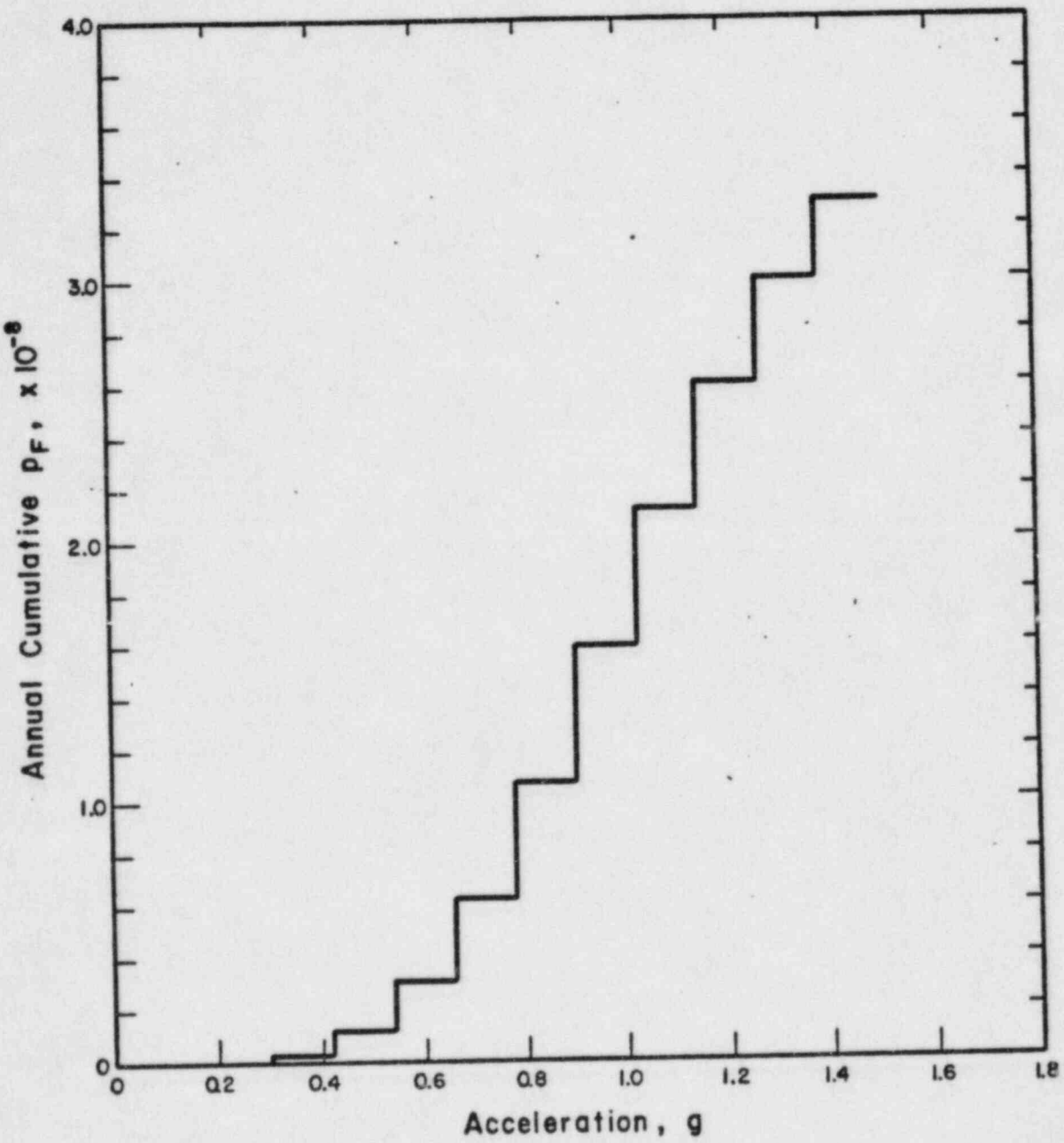

FIG. 10 INCREMENTAL CONTRIBUTIONS TO DAMAGE PROBABILITY OF STRUCTURAL COMPONENT (SF=20)

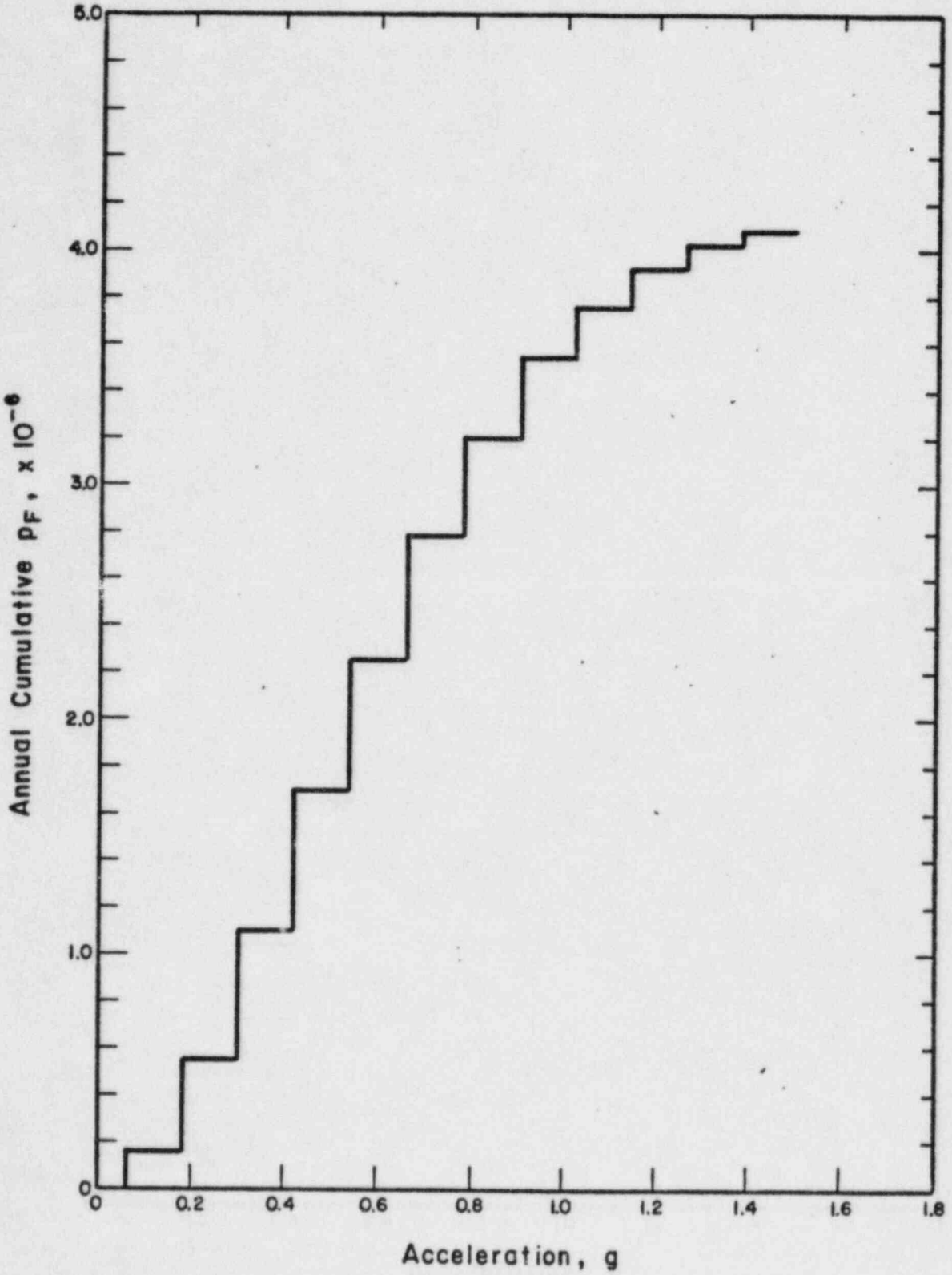

FIG. 11 INCREMENTAL CONTRIBUTIONS TO DAMAGE PROBABILITY OF PIPING SYSTEM (n = 1)

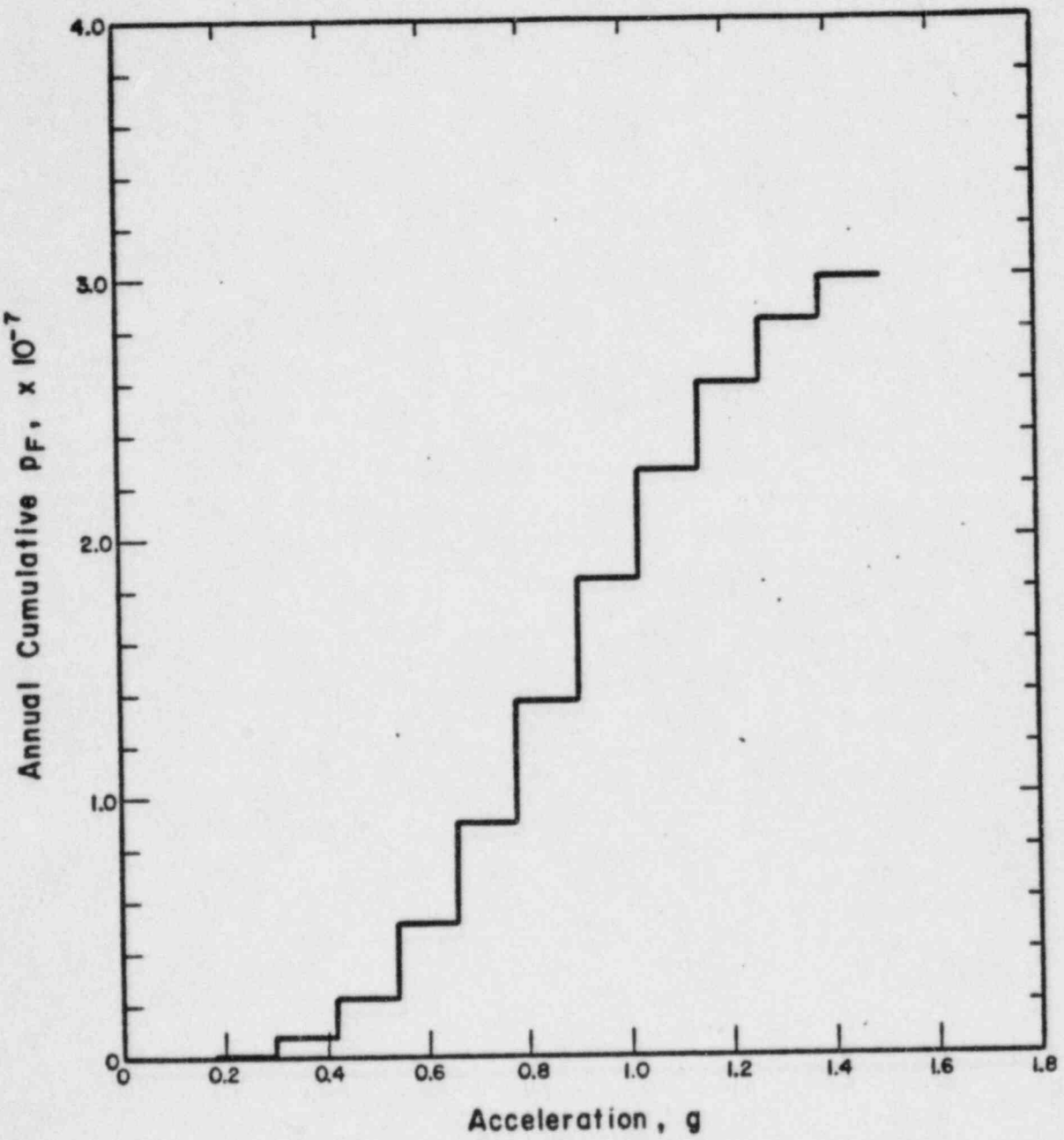

FIG. 12 INCREMENTAL CONTRIBUTION TO PIPING AND LIGHT EQUIPMENT DAMAGE PROBABILITY (n = 1)